

Interlayer binding energy of graphite: A mesoscopic determination from deformationZe Liu,¹ Jefferson Zhe Liu,^{2,*} Yao Cheng,³ Zhihong Li,⁴ Li Wang,⁵ and Quanshui Zheng^{1,5,†}¹*Department of Engineering Mechanics and Center for Nano and Micro Mechanics, Tsinghua University, Beijing 100084, China*²*Department of Mechanical and Aerospace Engineering, Monash University, Clayton, VIC 3800, Australia*³*Department of Engineering Physics, Tsinghua University, Beijing 100084, China*⁴*Institute of Microelectronics, Peking University, Beijing 100871, China*⁵*Institute of Advanced Study, Nanchang University, Nanchang, China*

(Received 19 April 2011; published 10 May 2012)

Despite the interlayer binding energy being one of the most important material properties of graphite, direct experimental determination of this property is yet to be reported. In this paper, we present an experimental method to directly measure the interlayer binding energy of highly oriented pyrolytic graphite (HOPG). The obtained value of the binding energy is $0.19 (\pm 0.01) \text{ J/m}^2$, which can serve as a benchmark for other theoretical and experimental works related to graphite/graphene systems.

DOI: [10.1103/PhysRevB.85.205418](https://doi.org/10.1103/PhysRevB.85.205418)

PACS number(s): 68.65.Pq, 68.35.Md

Since the successful fabrication of monolayer graphene from highly oriented pyrolytic graphite (HOPG) in 2004,¹ its perfect two-dimensional crystal, comprising carbon atoms, has become a topic of great interest. The superior electronic, thermal, and mechanical properties, along with the large specific surface area, make it a promising component in the next generation of electronic, energy storage and conversion, water treatment, and smart (bio)materials devices.^{2–5} Due to its inherent single layer structure, the direct application of graphene, to a large extent, requires a detailed understanding and control of its interactions with its surroundings.⁶ At present, the nature and strength of the interlayer binding in graphitic materials is poorly understood, despite the binding strength of graphite/graphene being directly relevant to many key applications; for example, graphene electronic devices fabricated upon various substrates, graphite intercalation compounds in Li batteries, carbon-based systems for hydrogen storage, and graphene-based supercapacitors.

The direct experimental measurement of the graphite interlayer binding energy (BE) and exfoliation energy (EE, the energy required to remove one graphene layer from single-crystalline graphite) is yet to be reported.⁷ It is well known that EE is smaller than BE, but the exact difference remains unknown. Although there are a few reported values that were obtained indirectly, these values are quite discrepant. Based on the heat of wetting data, Girifalco *et al.*⁸ reported the EE value as $0.26 \pm 0.03 \text{ J/m}^2$ (or $43 \pm 5 \text{ meV/atom}$). Based on collapsed carbon nanotube measurements, Benedict *et al.*⁹ extrapolated the BE to $0.21 (+0.09, -0.06) \text{ J/m}^2$ [or $35 (+15, -10) \text{ meV/atom}$]. More recently, Zacharia *et al.*¹⁰ performed desorption experiments of aromatic molecules on a graphite surface and obtained the approximate graphite EE of $0.32 \pm 0.03 \text{ J/m}^2$ (or $52 \pm 5 \text{ meV/atom}$, which yields an estimated BE of 0.37 J/m^2).

Theoretically, the ability to model the BE and EE for graphite is still under scrutiny due to the weak van der Waals interlayer binding, which remains notoriously difficult to describe within standard density functional theory (DFT).^{7,11} The standard approximations used in DFT, such as the local density approximation (LDA) and generalized gradient approximation (GGA), cannot accurately describe long-distance interactions

such as that of the van der Waals force. An alternative to standard DFT is the van der Waals density functional method, which was developed to account for the long-range interaction component by using an explicit nonlocal functional of the density. Use of this method yields, however, very scattered BE values of 0.15 J/m^2 (or 24 meV/atom), 0.28 J/m^2 (or 45.5 meV/atom), and 0.30 J/m^2 (or 50 meV/atom),^{12–14} and predicts substantially higher interlayer distance than the experimental value (e.g., 0.36, 0.376, vs 0.334 nm) and significantly lower C_{33} elastic modulus (e.g., 13, 27 vs 36 GPa). Very recently, two comprehensive first-principle studies predicted the BE of graphite. Spanu *et al.*⁷ employed the quantum Monte Carlo method to obtain a graphite BE of about 0.34 J/m^2 (or 56 meV/atom), and Lebegue *et al.*¹¹ used the adiabatic-connection fluctuation-dissipation theorem in the direct random approximation to obtain a BE of 0.29 J/m^2 (or 47 meV/atom).

The above review demonstrates a clear need for the direct experimental determination of the BE for graphite. In this paper, we introduce a method to directly measure the BE of a layered material, which is motivated by our recent discovery of a self-retraction phenomenon in micrometer graphite flakes sheared from graphite mesas.¹⁵ The idea is to assemble a thin graphite flake so that it spans a graphite step (Fig. 1). The top and bottom graphite flakes under consideration consist of multilayered graphenes assembled in an *AB* stacking configuration. The van der Waals interactions between the top and bottom HOPG flakes are represented by a series of nonlinear springs in Fig. 1. The key to this experimental technique is to create a graphite flake and a graphite step with atomically smooth surfaces and assemble them together. In our experiments, the top surface of each graphite flake was coated with a SiO_2 thin film. The total free energy of this system includes elastic deformation energy of the top graphite/ SiO_2 flake and the energy of the exposed graphite surfaces between the top flake and bottom mesa (related to the BE of graphite). Equilibrium of the system requires the minimization of the total free energy. In principle, given the geometry, such as step height, the thicknesses of the SiO_2 film, and the graphite flake, and the material elastic constants, the deformation of the top graphite/ SiO_2 flake should be solely determined by

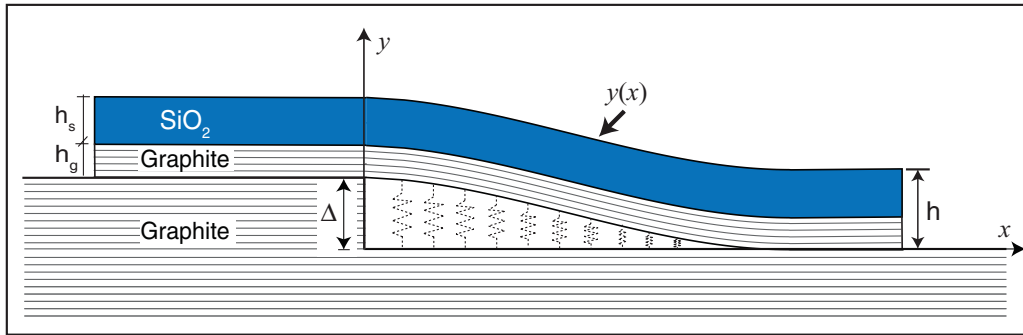


FIG. 1. (Color online) Sketch of a graphite/SiO₂ flake spanned a graphite step of height Δ with the deflection curve of top flake denoted as $y(x)$. The deformation of the top flake is caused by the van der Waals interactions between the top graphite flake and the bottom HOPG step, which are represented by a sequence of nonlinear springs. Measuring the deflection curve in experiments can determine the binding energy of HOPG.

the binding energy of the graphite. By combining atomic force microscope (AFM) measurement on the deflection profiles of the top flakes and finite element analysis (FEA), we determine the binding energy of graphite as $0.19 \pm 0.01 \text{ J/m}^2$ (or $31 \pm 2 \text{ meV/atom}$). The details of our experiments and analysis are reported below.

The HOPG samples were purchased from Veeco (ZYH grade). As illustrated in Fig. 2(a), graphite mesas were fabricated by using the same technique as that reported in Ref. 15. After mechanical exfoliation, a clean and fresh top surface of the HOPG sample was obtained. A SiO₂ film was then grown on the top surface of the sample via plasma enhanced chemical vapor deposition (PECVD), followed by electron-beam lithography and reactive ion etching. Figures 2(b) and 2(c) shows the scanning electron microscope (SEM, FEI Quanta 200F) image of the side view of two typical

mesas as the sample stage tilted 50°, one for a fabricated mesa and the other for a sheared mesa.

Similar to Ref. 15, we employed a micromanipulator MM3A (Kleindiek) that had been set in SEM (FEI Quanta 200F) to perform our experiments under a high-vacuum environment ($1.19\text{--}6.72 \times 10^{-4} \text{ Pa}$) at room temperature. An electron beam with 30-kV acceleration and 3-nm spot size was used to monitor the fabrication process. The *in situ* process can be seen in the Supplemental Material.¹⁶ Schematically we show the experimental process in Fig. 3. We placed the microprobe on the top surface of a selected mesa and then pushed it in a lateral direction [Fig. 3(a)]. A graphite/SiO₂ flake was then sheared out from its platform (base flake of the graphite mesa). The flake was found to be fully self-retractable after removing the microprobe. Our study on the self-retraction mechanism has revealed that

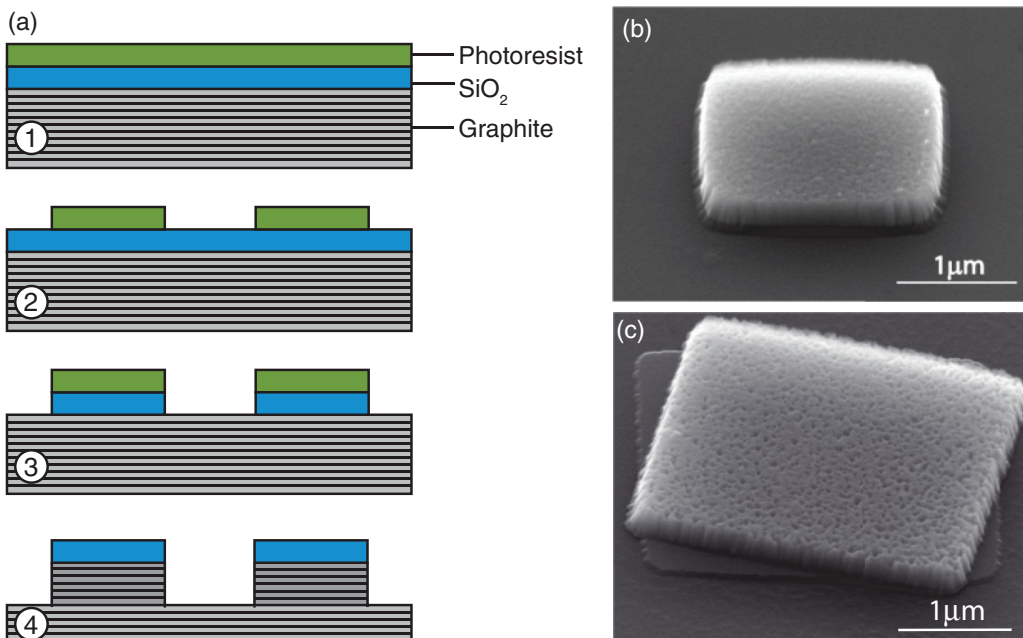


FIG. 2. (Color online) (a) Fabrication of graphite mesas. SiO₂ thin film is grown on top of the mesa by using plasma enhanced chemical vapor deposition. Electron-beam lithography and reaction ion etching is then used to fabricate the mesa. (b),(c) Scanning electron microscopy image of the side view of the fabricated mesas as the sample stage tilted 50°, one for a fabricated mesa and the other for a sheared mesa.

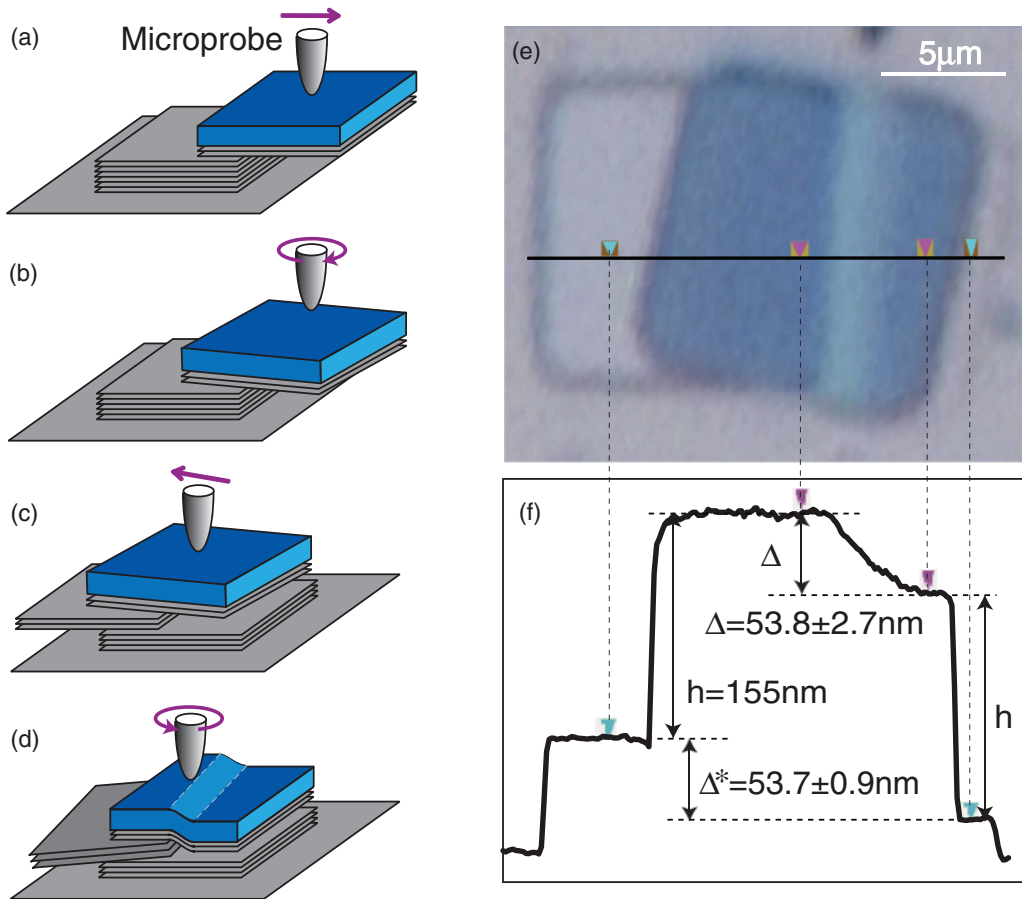


FIG. 3. (Color online) Illustration of the experimental process. (a) A microprobe is used to slide a graphite/SiO₂ flake with respect to the bottom flake. (b) The graphite/SiO₂ flake is then rotated by a certain angle to a lockup state (see text and Supplemental Material, Ref. 16). (c) After that the tip is moving in the opposite direction to split the slid flake into two parts: top and middle flake. (d) The top flake is spanned over the middle and bottom flakes and then it is rotated by the MM3A tip to another lockup state. (e) The optical microscope image of one obtained sample. (f) The profile obtained by atomic force microscopy (AFM) indicates that the adhesion has indeed taken place. The blue color in (e) reveals the constructive interference of $\sim\lambda/2$ (130 nm) thickness of SiO₂ layer, that is consistent with the measurement in (f). The appearance of a greenish blue band in (e) reveals that the slope surface is quite uniform in width direction.

the slipping plane corresponds to a boundary between two single-crystal graphite grains and that the original assembly between the displaced flake and the platform (before shear) is not *AB* stacked, which leads to large-scale superlubricity^{15,17} and consequently the self-retraction motion. To prevent self-retraction, we used the microprobe to rotate the flake through a certain angle until it suddenly locked up, which corresponds to an *AB*-stacking assembly as revealed by our recent study.¹⁷ In the experiment, pushing the locked top flake again in the opposite lateral direction leads to the separation of the flake into two parts: the top and the middle flakes. The observed self-retraction between these two separated flakes (see Supplemental Material¹⁶) is again indicative of non-*AB* stacking. To prevent the self-retraction, we rotated the top flake with respect to middle flake to another lockup state [Fig. 3(d)], so that the two flakes over the platform were both locked up.

An optical microscope (OM, HiRox KH-3000) image of a typical locked-up example in our experiments is shown in Fig. 3(e), where the top flake (blue colored) spanned the middle graphite flake. Figure 3(f) shows the height profile

along the black line in Fig. 3(e), obtained using an atomic force microscope (AFM). The measured step height, which equates to the middle flake thickness, is $\Delta^* = 53.7 \pm 0.9$ nm. In comparison, the height drop along the top flake surface was measured as $\Delta = 53.8 \pm 2.7$ nm, which is almost the same as the thickness of the middle flake. Such a good agreement confirms the strong adhesion of the top flake with the middle flake and the platform. This negligible difference could arise from the surface roughness of the SiO₂ thin film. The strong adhesion is also supported by the color image in Fig. 3(e), where the blue color is fully reproduced at both of the flat sides on the top flake.

We also prepared four samples in SEM under high-vacuum condition using a similar procedure as that explained before. Figure 4(a) shows the AFM measured height profiles along the lines in the inset figure for one typical sample. The thickness of the top flake is measured as $h = 239 \pm 2$ nm and the height of the step (i.e., the thickness of the middle flake) is $\Delta = 51 \pm 1$ nm. Using the MM3A micromanipulator to take the top flake off its platform and then stand the flake up, we measured the thickness of the SiO₂ film as

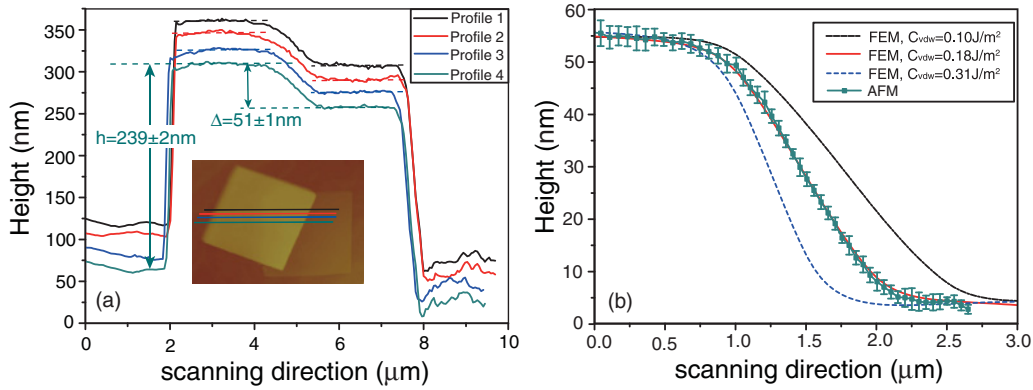


FIG. 4. (Color online) AFM height profiles along the colored lines in inset of a double locked-up sample prepared in SEM in a high-vacuum condition. These profiles are shifted for visualization clarity. (b) Comparison of AFM average scanned height profiles of the top flake with those calculated from FEM models. A set of binding energy values is tried in our FEM model (see text and Supplemental Material in Ref. 18 for details). It is clear for this sample that binding-energy value 0.18 J/m^2 has the best agreement.

157 nm (sample 1 in Fig. S2 of Supplemental Material, Ref. 18). As explained earlier, the deformation of the top flake is determined by the geometries, the elastic constants of SiO_2 and graphite, and the van der Waals interactions (i.e., binding energy) between the graphite layers, which remain to be determined. We use a finite-element model [FEM, see details in Supplemental Material, Ref. 18] to simulate the deflection of the top graphite/ SiO_2 flake. Nonlinear spring elements are used to mimic the van der Waals interactions, with force-displacement relation derived from the Lennard-Jones potential $V(r) = 4\epsilon[(\sigma/r)^{12} - (\sigma/r)^6]$. We fixed $\sigma = 0.3415 \text{ nm}$ ¹⁹ and tried different ϵ (i.e., accordingly a set of trial binding energy values) to calculate the equilibrium deflection curves and then compared them with the AFM measurement. The best fitting should yield the binding energy value. One example of such fitting is given in Fig. 4(b). The symbols are the average of six AFM scans depicted in Fig. 4(a). The smooth curves represented the calculated deflections from our FEM model with the different trial binding-energy values as denoted. From Fig. 4(b), we can estimate that the BE value is about 0.18 J/m^2 . Using the same method for the other three samples prepared in SEM, we have determined the BE values 0.19 , 0.20 , 0.18 J/m^2 , respectively. Details of the AFM measurements and FEM models are provided in the Supplemental Material.¹⁸ The average value of binding energy is $0.19 \pm 0.01 \text{ J/m}^2$.

It is known that chemisorption, physisorption, and insertion of gases inside graphite can drastically change the surface/interface properties.²⁰ The BE of graphite under vacuum was estimated to be approximately 100 times greater than those in an environment with air, oxygen, or water vapor.²¹ To avoid contamination caused by adsorption, we note again that our reported experiments are carried out within SEM with high-vacuum condition ($\sim 10^{-4} \text{ Pa}$). Similar experiments, but in open-air conditions, were also conducted as shown in Fig. 3. Through similar analysis, the BE values determined in the open-air condition is smaller but still comparable to that measured inside SEM, 0.08 J/m^2 . This result gives an additional support that the self-retraction motion of graphite/ SiO_2 flakes can very well self-clean the adsorbate on the exposed sliding surfaces.²²

Exposing a fresh graphite surface to an electron beam in SEM (30 kV acceleration with 3 nm spot size) could cause carbon deposition and thus could affect the atomically smooth contact between top and bottom graphite flakes. Our experimental process [from Fig. 3(c) to Fig. 3(d)] was carefully designed so that the contact interface was always covered by the top flake and protected from the electron beam irradiation.¹⁶ We believe the electron-beam induced carbon deposition in the contact interface is negligible.

Potential interface defect (such as steps, etc.) is another detrimental factor for the BE measurements. Our method overcomes this problem as well. In preparing our samples, we found that we needed to deliberately rotate the top flake [Figs. 3(b) and 3(d)]; otherwise the self-retraction would occur. Our recent experimental studies revealed that a necessary condition for such self-retraction motion is an atomically smooth interface.¹⁷ Indeed, the height profiles of our STM scans on a typical contact interface of a self-retractable graphite flake are smooth with a variation of only 0.5 nm over a scanning length of $1.5 \mu\text{m}$.¹⁷ We believe that atomic steps should have a negligible effect in our experiments. This is also consistent with our HOPG crystal structure. By using electron-backscattered diffraction (EBSD) to study the free surface of the same type of HOPG used to create the mesas, we measured the size distribution of the grains (that are rotationally misoriented relative to each other). The grain size is in the range of $3\text{--}60 \mu\text{m}$ with the average about $13 \mu\text{m}$.¹⁷ This distribution implies that the probability of atomic steps and other defects that occurs usually at grain boundaries should be very small in our mesas of linear dimension $< 5 \mu\text{m}$.

In summary, we have presented a experimental method to directly measure the interlayer BE of graphite. The herein measured BE for HOPG was $0.19 \pm 0.01 \text{ J/m}^2$ (or $31 \pm 2 \text{ meV/atom}$). In comparison to other indirect experimental methods, the key is to create an atomically smooth interface with contact area on the order μm^2 prepared in high-vacuum condition, to minimize the detrimental effects of surface contamination and atomic defects. Our experiments provided a direct and reliable determination on the binding energy of HOPG. The determined binding energy can serve as a useful

benchmark in understanding the van der Waals interactions in the prototypical material system: graphite. Our method can be easily extended to measure the binding energies between graphite/graphene and other types of substrates. It can also be used in other systems, particularly lamellar materials and thin films. Considering the difficulty in measuring the interfacial BE in micro/nanomaterials, our method could serve as a general solution to this problem.

Q.S.Z. acknowledges the financial support from NSFC through Grant No. 10832005, the National Basic Research Program of China (Grant No. 2007CB936803), and the National 863 Project (Grant No. 2008AA03Z302). J.Z.L. acknowledges Small Grant 2011 and Seed Grant 2012 from the engineering faculty of Monash University. Z.L. acknowledges F.H. Gao and Z.J. Lin for helpful discussions about the FEM model.

*zhe.liu@monash.edu

†zhengqs@tsinghua.edu.cn

¹K. S. Novoselov, A. K. Geim, S. V. Morozov, D. Jiang, Y. Zhang, S. V. Dubonos, I. V. Grigorieva, and A. A. Firsov, *Science* **306**, 666 (2004).

²A. K. Geim, *Science* **324**, 1530 (2009).

³A. K. Geim and K. S. Novoselov, *Nat. Mater.* **6**, 183 (2007).

⁴M. D. Stoller, S. J. Park, Y. W. Zhu, J. H. An, and R. S. Ruoff, *Nano Lett.* **8**, 3498 (2008).

⁵N. Mohanty and V. Berry, *Nano Lett.* **8**, 4469 (2008).

⁶X. Du, I. Skachko, A. Barker, and E. Y. Andrei, *Nat. Nanotechnol.* **3**, 491 (2008).

⁷L. Spanu, S. Sorella, and G. Galli, *Phys. Rev. Lett.* **103**, 196401 (2009).

⁸L. A. Girifalco and R. A. LAD, *J. Chem. Phys.* **25**, 693 (1956).

⁹L. Benedict, N. G. Chopra, M. L. Cohen, A. Zettl, S. G. Louie, and V. H. Crespi, *Chem. Phys. Lett.* **286**, 490 (1998).

¹⁰R. Zacharia, H. Ulbricht, and T. Hertel, *Phys. Rev. B* **69**, 155406 (2004).

¹¹S. Lebegue, J. Harl, T. Gould, J. G. Angyan, G. Kresse, and J. F. Dobson, *Phys. Rev. Lett.* **105**, 196401 (2010).

¹²M. Dion, H. Rydberg, E. Schroder, D. C. Langreth, and B. I. Lundqvist, *Phys. Rev. Lett.* **92**, 246401 (2004).

¹³E. Ziambaras, J. Kleis, E. Schroder, and P. Hyldgaard, *Phys. Rev. B* **76**, 155425 (2007).

¹⁴S. D. Chakarova-Kack, E. Schroder, B. I. Lundqvist, and D. C. Langreth, *Phys. Rev. Lett.* **96**, 146107 (2006).

¹⁵Q. Zheng, B. Jiang, S. Liu, J. Zhu, Q. Jiang, Y. Weng, L. Lu, S. Wang, Q. Xue, and L. Peng, *Phys. Rev. Lett.* **100**, 067205 (2008).

¹⁶See Supplemental Material at <http://link.aps.org/supplemental/10.1103/PhysRevB.85.205418> for an *in situ* SEM movie.

¹⁷Z. Liu, J. Z. Liu, J. Yang, Y. Liu, Y. Wang, Y. Yang, and Q.-S. Zheng, e-print [arXiv:1104.3320v1](https://arxiv.org/abs/1104.3320v1), *Phys. Rev. Lett.* (to be published).

¹⁸See Supplemental Material at <http://link.aps.org/supplemental/10.1103/PhysRevB.85.205418> for nano-indentation experiments to measure the elastic modulus of SiO₂, our finite-element models for the BE determination, and discussion on effects of surface roughness and thermal residual stress.

¹⁹L. A. Girifalco, M. Hodak, and R. S. Lee, *Phys. Rev. B* **62**, 13104 (2000).

²⁰H. Zaidi, F. Robert, and D. Paulmier, *Thin Solid Films* **264**, 46 (1995).

²¹P. J. Bryant, *Mechanics of Solid Friction* (Elsevier, Amsterdam, 1964).

²²Z. Liu, P. Boggild, J. R. Yang, Y. Cheng, F. Grey, Y. L. Liu, L. Wang, and Q.-S. Zheng, *Nanotechnology* **22**, 265706 (2011).